American Mineralogist, Volume 102, pages 2333–2340, 2017

Charleshatchettite, $CaNb_4O_{10}(OH)_2 \cdot 8H_2O$, a new mineral from Mont Saint-Hilaire, Québec, Canada: Description, crystal-structure determination, and origin

Monika M.M. Haring[1,*] and Andrew M. McDonald[1]

[1]Department of Earth Sciences, Laurentian University, Sudbury, Ontario P3E 2C6, Canada

Abstract

Charleshatchettite, $CaNb_4O_{10}(OH)_2 \cdot 8H_2O$, is a new mineral related to franconite and hochelagaite, discovered on a fracture surface of a nepheline syenite at Mont Saint-Hilaire, Québec, Canada. The mineral occurs in white globules (~0.15–0.20 mm in diameter) composed of radiating crystals with individual crystals having average dimensions of ~0.002 × 0.010 × 0.040 mm. Crystals are euhedral, bladed (flattened on [100]), and are transparent to translucent. The mineral is associated with albite, quartz, muscovite, pyrrhotite, pyrite, ancylite-(Ce), and siderite. Charleshatchettite is inferred to be biaxial (–) with $\alpha' = \sim 1.72(2)$ and $\gamma' = \sim 1.82(2)$. Data from chemical analyses (SEM-EDS, $n = 8$): CaO 7.96 (7.04–8.63), MgO 0.24 (0.08–0.78), Al_2O_3 0.13 (b.d.–0.49), SiO_2 1.04 (0.49–1.88), TiO_2 3.64 (2.45–5.05), Nb_2O_5 68.07 (64.83–71.01), and H_2O (calc) 22.96, total 104.04 wt% gives the average empirical formula: $(Ca_{1.00}Mg_{0.04})_{\Sigma 1.04}(Nb_{3.62}Ti_{0.32}Si_{0.12}Al_{0.02})_{\Sigma 4.08}O_{10}(OH)_2 \cdot 8H_2O$ (based on 20 anions). This is similar to that of hochelagaite ($CaNb_4O_{11} \cdot nH_2O$), although the two are readily distinguished by their powder X-ray diffraction patterns. Results from single-crystal X-ray diffraction analysis give $a = 21.151(4)$, $b = 6.496(2)$, $c = 12.714(3)$ Å, and $\beta = 103.958(3)°$, space group $C2/c$ (no. 15). The crystal structure, refined to $R = 5.64\%$, contains 1 *Ca* site, 2 distorted octahedral Nb sites, and 10 O sites. It consists of clusters of four edge-sharing $Nb(O,OH)_6$ octahedra, linked through shared corners to adjacent clusters, forming layers of $Nb(O,OH)_6$ octahedra. These alternate along [100] with layers composed of $Ca(H_2O)_8$ polyhedra, the two being linked together by H-bonding. Charleshatchettite is a late-stage mineral, interpreted to have developed through the interaction of low-T (<150 °C) aqueous fluids with an alkali-, Nb-rich precursor under slightly reducing conditions and a highly alkaline pH. The precursor mineral(s) is unknown but is considered to have been Nb-dominant, relatively unstable under slightly reducing as well as alkaline conditions, and likely itself would have been a product of near-complete Nb/Ta fractionation due to the paucity of Ta in charleshatchettite. Charleshatchettite is crystallochemically related to Sandia Octahedral Molecular Sieves [SOMS; $Na_2Nb_{2-x}M_xO_{6-x}(OH)_x \cdot H_2O$ with M = Ti, Zr, Hf], a group of synthetic compounds with strong ion exchange capabilities.

Keywords: New mineral, charleshatchettite, Mont Saint-Hilaire, SOMS, hochelagaite, franconite, Nb/Ta fractionation, crystal structure

Introduction

Franconite-group minerals (FGM) are alkali-niobate hydrates that develop as late-stage, low-T minerals in agpaitic environments including Mont-Saint Hilaire (Horváth and Gault 1990), the Saint-Amable sill (Horváth et al. 1998), the Khibiny massif (Pekov and Podlesnyi 2004), the Vuoriyarvi alkaline-ultrabasic massif (Belovitskaya and Pekov 2004), and the Vishnevogorsk alkali complex (Nikandrov 1990). Current members of the FGM include franconite [$Na(Nb_2O_5)(OH) \cdot 3H_2O$], hochelagaite ($CaNb_4O_{11} \cdot nH_2O$; Jambor et al. 1986), and ternovite ($MgNb_4O_{11} \cdot nH_2O$; Subbotin et al. 1997). The crystal structures and chemical formulas of these minerals are in general, difficult to resolve, primarily owing to their occurrence in thin (<5 μm) blades, but also because these typically develop into more complex, radiating spheres wherein more than one species may be present. Despite obvious challenges, progress has been made in unraveling the crystal-chemical structures of the FGM, mainly due to advances having been made in single-crystal X-ray diffraction methods. For example, the crystal structure of franconite was solved by Haring and McDonald (2014) who showed the mineral is strongly layered with sheets of $Nb(O,OH)_6$ polyhedra alternating with sheets $Na(O,H_2O)_5$ polyhedra, these being joined by weak H-bonds along [100], and provided a refined chemical formula $Na(Nb_2O_5)(OH) \cdot 3H_2O$. The crystal structures of hochelagaite and ternovite still remain unsolved but a combination of data from PXRD and Raman/FTIR spectroscopy suggest they are all closely related.

As part of a broader study aimed at better understanding the development of late-stage niobate minerals from agpaitic environments, an investigation of a previously undescribed species believed to be related to minerals of the FGM, was undertaken. This mineral, which serves as the subject of this report, was likely first observed in specimens ($n = 5$) collected by Elsy and Les Horváth in 1978. It was not recognized as a potentially new species until 1985, based on material ($n = 2$) collected in

* E-mail: mharing53@gmail.com

the Poudrette Quarry at Mont Saint-Hilaire, Québec, by the late Ron Wadell. The material was found to be a Ca-niobate hydrate, chemically similar to hochelagaite, but with a PXRD pattern distinct from that of the former; it was thus considered as potentially being a new mineral species and given the temporary designation UK56. The very thin nature of its crystals (~0.002 mm on average) and evidence for stacking disorder (e.g., X-ray precession images) precluded a complete analysis by single-crystal methods available and so it remained an unidentified mineral for a considerable period of time. However, the advent of extremely bright X-ray sources arising from a combination of rotating-anode generators coupled with multi-layer optics, incident-beam paths, and highly sensitive detectors, has proved invaluable in solving the crystal structures of minerals whose crystal structures would have formerly been challenging if not impossible to solve (Cooper and Hawthorne 2012). An example of just how critical this technology has become is shown in this study of UK56, which is now recognized as the new species, charleshatchettite, $CaNb_4O_{10}(OH)_2 \cdot 8H_2O$.

In this contribution, we present and discuss data pertaining to the crystal chemistry of charleshatchettite, elucidate the relationship of the mineral to other members of the FMG, describe the geological conditions under which it is thought to have developed, and compare it to synthetic niobate compounds such as Sandia Octahedral Molecular Sieves (SOMS). The mineral is named in recognition of Charles Hatchett (1765–1847), an English chemist who discovered niobium, a dominant element in charleshatchettite. Both the mineral and mineral name have been approved by the Commission on New Minerals, Nomenclature and Classification of the International Mineralogical (2015-048). The holotype material is housed in the collections of the Canadian Museum of Nature, Gatineau, Québec, under catalog number CMNMC 86894.

Occurrence

Charleshatchettite was discovered on a fracture surface on a fine-grained nepheline syenite at the Poudrette quarry, La Vallée-du-Richelieu, Montérégie (formerly Rouville County), Québec, Canada (45°33′8″N, 73°9′3″W). Associated minerals include (in order of decreasing modal abundance) albite, quartz, muscovite, pyrrhotite, pyrite, ancylite-(Ce), and siderite. The mineral has only been found on two samples to date. Owing to the similarity in appearance and physical properties of charleshatchettite to other FGM, the mineral may be present other specimens labeled as hochelagaite or franconite. The fracture surface upon which charleshatchettite occurs is dominated by translucent, white, subhedral, blocky crystals of albite (average dimensions: 0.7 × 1.5 × 2 mm). These are intergrown with transparent crystals of euhedral quartz displaying the forms prism {120} and dipyramid {112} (average dimensions: 0.9 × 0.8 × 1.5 mm). Both the quartz and the albite are overgrown by euhedral, colorless, platy crystals of muscovite, which can also be found intergrown with anhedral crystals of pyrrhotite. The pyrrhotite is strongly magnetic, suggesting that it is likely the monoclinic 4*C* polytype, possibly suggesting a *T* of formation <230 °C (Kontny et al. 2000). The pyrrhotite is overgrown by euhedral crystals of pyrite displaying the cube {100} and octahedron {111}. Siderite overgrows both the pyrrhotite and the pyrite and can show rusty staining. It develops as euhedral rhombohedra {111} that are tan to light brown (average dimensions 1.0 × 0.8 × 1.2 mm). Rare, euhedral, light pink crystals ancylite-(Ce) (average dimensions: 0.4 × 0.5 × 0.8 mm) overgrow muscovite and pyrrhotite. The associated ancylite-(Ce) is characterized by a bluish-gray fluorescence when exposed to long-, medium-, and short-wave radiation. Charleshatchettite is paragentically the last mineral to develop and can be found overgrowing all the other associated minerals. The general paragenetic sequence involving charleshatchettite is given in Figure 1.

Physical properties

Charleshatchettite occurs in white globules ~0.15 to 0.20 mm in diameter, composed of radiating crystals (Fig. 2). Individual crystals have average dimensions of ~0.07 × 0.02 × 0.01 mm and are euhedral, bladed with a perfect [100] cleavage. They are white, transparent to translucent, with a silky luster, and are flattened on [100] and elongated along [001]. Charleshatchettite, like hochelagaite, does not exhibit fluorescence under long-, medium-, or short-wave radiation; this is in contrast with franconite that typically exhibits a distinctive bright yellow-white fluorescence under short-wave and a dull yellow-white fluorescence under long-wave radiation (Horváth and Gault 1990). The Mohs hardness could not be determined due to the small sizes of the crystals. Hochelagaite was estimated to have a Mohs hardness of ~4 and given the crystal-chemical similarities between hochelagaite and charleshatchettite, charleshatchettite likely has a similar hardness. A density of 2.878 g/cm^3 was calculated using the empirical chemical formula and unit-cell parameters derived from the crystal-structure analysis.

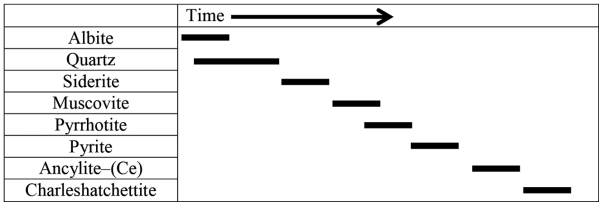

Figure 1. Mineral paragenesis for charleshatchettite.

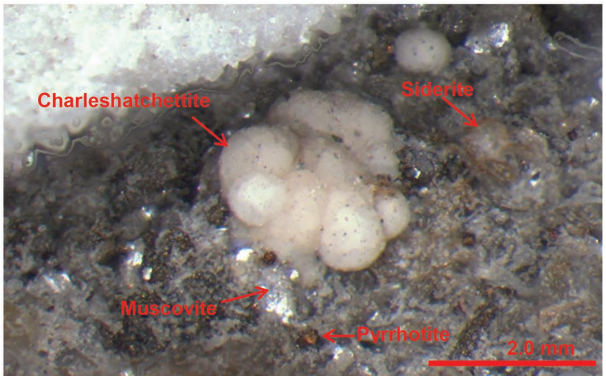

Figure 2. Globules of charleshatchettite with muscovite, siderite, and pyrrhotite. (Color online.)

A complete set of optical data as well as an interference figure could not be measured due to the thinness (~1 μm) of the crystals the *b*-axis. The mineral is assumed to be biaxial due to the fact it is monoclinic. It has $\alpha' = \sim 1.72(2)$ perpendicular to the plane of the blades and $\gamma' = \sim 1.82(2)$ along the length of the crystals. These values are similar to those of other FGM including hochelagaite [$n_{min} = 1.72(2)$ and $n_{max} = 1.82(2)$; Jambor et al. 1986], franconite [$n_{min} = 1.72(2)$ and $n_{max} = 1.79(2)$; Jambor et al. 1984], and ternovite [$n_{min} = 1.72(2)$ and $n_{max} = 1.85(2)$; Subbotin et al. 1997]. The mineral is assumed to be optically negative as it has unit-cell parameters and refractive indices similar to other FGM, which are optically negative. Charleshatchettite is colorless under plane-polarized light with no observed pleochroism. The compatibility index, calculated using the empirical formula and unit-cell parameters derived from the crystal-structure analysis, is 0.055, which is considered good (Mandarino 1981). A combination of the instability of the mineral under the electron beam (leading to elemental loss) and that only two refractive indices could be measured likely influence the less-than-ideal compatibility index.

Chemistry

Chemical analyses of charleshatchettite were made by energy-dispersive spectrometry with a JEOL JSM 6400 scanning electron microscope operated at a voltage of 20 kV, a beam current of ~1 nA, and a beam width of 1 μm. The following standards (X-ray lines) were employed: $CaTiO_3$ (Ca*K*α, Ti*K*α), diopside (Mg*K*α, Si*K*α), albite (Al*K*α), and synthetic $MnNb_2O_6$ (Nb*K*α). Four charleshatchettite-bearing globules were examined in this study and all were found to be a single-phase, i.e., free of other potential Na-dominant phases, including franconite. From the globules, five crystals of charleshatchettite were selected for analysis. Chemical analyses ($n = 8$) of these gave the average (range) compositions: CaO 7.96 (7.04–8.63), MgO 0.24 (0.08–0.78), Al_2O_3 0.13 (b.d.–0.49), SiO_2 1.04 (0.49–1.88), TiO_2 3.64 (2.45–5.05), Nb_2O_5 68.07 (64.83–71.01), and H_2O (calc) 22.96, total 104.04 wt% corresponding to the empirical formula: $(Ca_{1.00}Mg_{0.04})_{\Sigma 1.04}(Nb_{3.62}Ti_{0.32}Si_{0.12}Al_{0.02})_{\Sigma 4.08}O_{10}(OH)_2 \cdot 8H_2O$ (based on 20 anions) or ideally $CaNb_4O_{10}(OH)_2 \cdot 8H_2O$. There was insufficient material for direct analysis of H_2O, so the calculated H_2O is based on results from the crystal structure. The mineral was found to be highly unstable under the electron beam, so the high-analytical total may be attributed to water-loss during analysis. Additional elements, including Na, Ta, and F, were also sought, but not detected. The strongest EDS peak associated with Ta is located at *L*α 8.145 keV was absent in the EDS spectrum of charleshatchettite confirming the absence of Ta. Although there is some overlap between peaks in the EDS spectra of Si and Ta, there is a large difference in energy between the strongest peaks of each element (strongest peaks: Ta = *L*α 8.145 keV, Si = *K*α 1.739 keV). The notable absence of Ta, despite the crystal-chemical similarity of Ta and Nb, is consistent with analyses made of other Nb-dominant mineral from agpaitic environments, including those of the FGM (Haring and McDonald 2014).

Raman and infrared spectroscopy

The Raman spectrum of charleshatchettite was collected with a Horiba Jobin Yvon XPLORA Raman spectrometer interfaced with an Olympus BX41 microscope using a crystal mounted on a spindle stage and oriented such that the laser was perpendicular to {100}. The spectrum (Fig. 3a) represents an average of three 20 s acquisition cycles, each collected over a range of 50 to 4000 cm^{-1}. The mineral was first analyzed using an excitation radiation of $\lambda = 532$ nm but this was found to produce fluorescence peaks in the region of ~2500 cm^{-1}, a region that does not typically contain bands attributable to any chemical groups in most minerals. To evaluate this further, the mineral was instead analyzed using an excitation radiation of $\lambda = 638$ nm; this eliminated all peaks in the region, suggesting they were indeed products of fluorescence. A grating of 1200 lines/cm and a 40× long working distance objective were also used, producing a beam of diameter ~2 μm. Calibration was made using the 521 cm^{-1} line of a silicon wafer. The Raman spectrum of charleshatchettite shows bands in the regions of 2900–3600, 1400–1500, 1000–850, 670–475, and 470–50 cm^{-1} (Table 1) (Fig. 2a). The first region at 2900–3600 cm^{-1} contains three moderately sharp to broad, weak to moderate intensity peaks at 3314, 3046, and 2939 cm^{-1} that are attributed to O-H bending (Williams 1995). In the region of 1400–1500 cm^{-1}, a weak low-intensity peak occurs at 1459 cm^{-1}, ascribed to H-O-H bending. The region of 1000 to 850 cm^{-1} contains two strong, sharp peaks at 930–878 cm^{-1} that can be attributed to the symmetric stretching of Nb=O double bonds (Jehng and Wachs

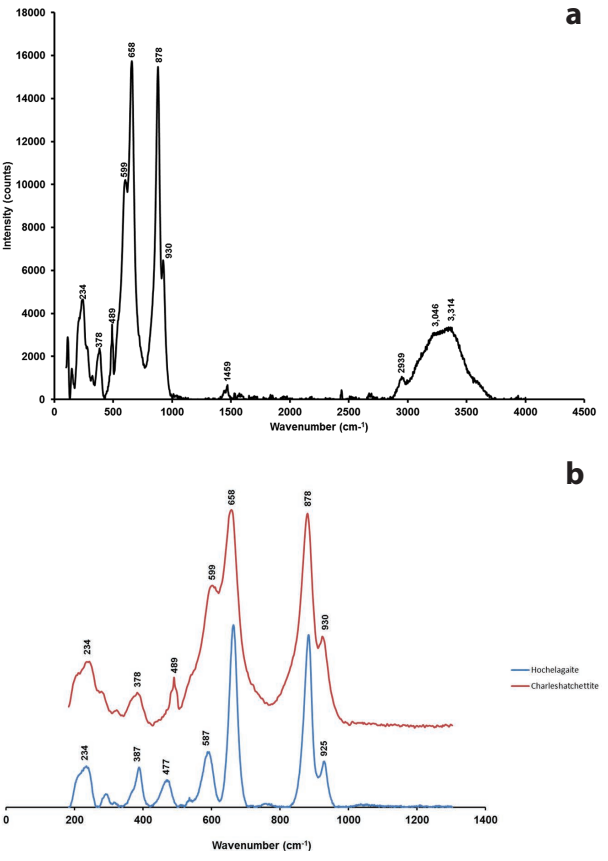

Figure 3. (**a**) Raman spectrum for charleshatchettite perpendicular to [100]. (**b**) Raman spectra for charleshatchettite and hochelagaite. (Color online.)

TABLE 1. Observed Raman absorption bands for charleshatchettite and hochelagaite

Hochelagaite[a]	Charleshatchettite				
Peak position (cm^{-1})	Peak position (cm^{-1})	Peak position calc. (cm^{-1})	Width	Intensity	Assignment
	3314		Broad	Mod. strong	O-H bending
	3046		Broad	Mod. strong	O-H bending
	2939		Mod. sharp	Weak	O-H bending
	1459		Mod. sharp	Weak	H-O-H bending
925	930	946	Sharp	Mod. strong	Symmetric stretching of Nb = O double bond
878	878	855	Sharp	Very strong	Symmetric stretching of Nb = O double bond
663	658	678	Sharp	Very strong	Nb-O-Nb linkages – symmetric stretching
587	599	607	Sharp	Mod. strong	Nb-O-Nb linkages – symmetric stretching
477	489	455	Mod. sharp	Weak	Ca-O
387	378	355	Mod. sharp	Weak	Ca-O
325	234	288	Sharp	Weak	Ca-O
300	215	–	Sharp	Mod. strong	Ca-O
234	205	183	Sharp	Weak	Ca-O
196	150	–	Mod. sharp	Weak	Ca-O
–	115	–	Sharp	Mod. strong	Ca-O

[a] Raman data for hochelagaite from this study.

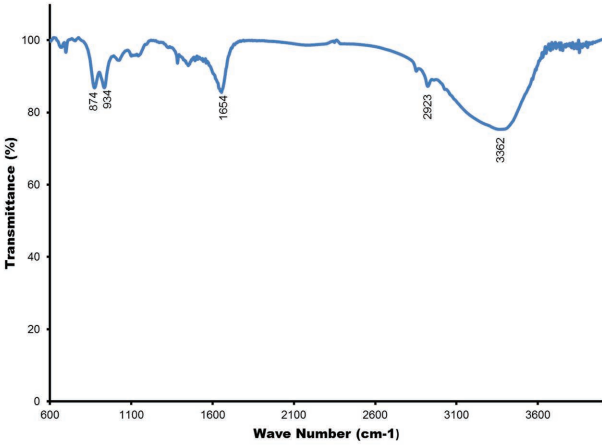

FIGURE 4. FTIR spectrum for charleshatchettite. (Color online.)

1990; Haring and McDonald 2014). The region between 670–475 cm^{-1} contains two strong sharp bands at 658 and 599 cm^{-1} that are attributed to symmetric stretching of Nb-O-Nb bonds (Jehng and Wachs 1990; Haring and McDonald 2014). Finally, the region at 470–50 cm^{-1} contains 7 low to moderate intensity peaks at 489, 378, 234, 215, 205, 150, and 115 cm^{-1} attributed to Ca-O bonds (Williams 1995). To confirm these band assignments, a Raman spectrum was calculated using results from the refined crystal structure (described below) along with the programs GAUSSIAN (Frisch et al. 2013) to calculate force constants for each bond, and VIBRATZ (Dowty 2009) to determine and refine the calculated Raman spectrum (Table 1). Results show an overall good agreement between the experimental and calculated Raman spectra in terms of both band position and intensity (Table 1). As a note, those peaks associated with O-H and H-O-H bending could not be determined for the calculated Raman spectrum owing to the fact that the site(s) occupied by H could not be reliably determined from the refined crystal structure. The Raman spectra for charleshatchettite and hochelagaite are compared in Figure 3b. These show that the spectra of the two minerals are virtually indistinguishable from one another; this is predictable, owing to strong chemical and crystal-structure similarities between the two. However, it does indicate that Raman spectroscopy cannot be used to reliably distinguish between them.

The presence of water in charleshatchettite was further investigated by infrared spectroscopy, given that water is a weak Raman scatterer but a strong absorber of infrared radiation. An infrared (FTIR) spectrum (Fig. 4) over the range of 600 to 4000 cm^{-1} was collected using a Bruker Alpha spectrometer equipped with a KBr beam splitter and a DTGS detector. This spectrum, obtained by averaging 128 scans with a resolution of 4 cm^{-1}, reveals three distinct bands in the regions of ~3700–2800, 1700–1300, and 1200–650 cm^{-1} (Table 2). The region at ~3700–2800 cm^{-1} consists of broad, high-intensity peak at 3362 cm^{-1} as well as two sharp, moderate intensity peaks at 2923 and 2852 cm^{-1} associated with O-H bending (Williams 1995). The second region at ~1700–1300 cm^{-1} consists of a sharp peak at 1654 and 1450 cm^{-1} as well as a sharp lower intensity peak at and 1384 cm^{-1} associated with H-O-H bending and atmospheric CO_2, respectively. The third region at 1200–650 cm^{-1} consists of two sharp, high-intensity peaks at 934 and 874 cm^{-1}, as well as lower intensity peaks at 1100, 1025, 755, and 697 cm^{-1}. The bands in this region are similar to those in the IR spectra of franconite [$Na(Nb_2O_5)(OH)\cdot 3H_2O$] with peaks at 1025, 934, and 874 cm^{-1} associated with possible Nb=O double bonds and the peaks at 755 and 697 cm^{-1} associated with Nb-O-Nb single bonds (Fielicke et al. 2003; Haring and McDonald 2014). The weak peak at 1100 cm^{-1}, attributed to a Si-O asymmetric stretch, is considered to be due to trace amounts of silicates such as quartz or albite, both of which are associated with charleshatchettite. There is overall good agreement between the complementary Raman and FTIR spectra collected for charleshatchettite. The low-intensity peak observed at 1459 cm^{-1} in the Raman spectrum of charleshatchettite, attributed to H-O-H bending, corresponds to the peak at

TABLE 2. FTIR peaks and peak assignments for charleshatchettite

FTIR transmittance band (cm^{-1})	Suggested assignment
3362	O-H bending
2923	O-H bending
2852	O-H bending
1654	H-O-H bending
1450	H-O-H bending
1384	Atmospheric CO_2
1100	Asymmetric Si-O stretching
1025	Symmetric stretching of Nb=O double bond
934	Symmetric stretching of Nb=O double bond
874	Symmetric stretching of Nb=O double bond
755	Nb-O-Nb linkages; symmetric stretching
697	Nb-O-Nb linkages; symmetric stretching
666	Nb-O-Nb linkages; symmetric stretching

1450 cm^{-1} in the FTIR spectrum. Other bands observed in the Raman spectrum of charleshatchettite that correspond to those present in the FTIR spectrum include those in the regions of 2900–3600 cm^{-1} (O-H bending) as well as 1000–850 (Nb=O bonds). However, given the chemical and structural similarities among FGM, the Raman spectra of these minerals are virtually identical, all with two sharp, strong peaks in the regions of 1000–850 and 670–475 cm^{-1} (Nb-O bonds) as well as a broad peak in the region of 2900–3600 cm^{-1}.

X-RAY CRYSTALLOGRAPHY AND CRYSTAL-STRUCTURE DETERMINATION

X-ray powder diffraction data were collected using a 114.6 mm diameter Gandolfi camera, a 0.3 mm collimator, and Fe-filtered Co*K*α radiation (λ = 1.7902 Å). Intensities were determined using a scanned image of the pattern and normalized to the measured intensity of d = 10.308 Å (I = 100). The measured intensities were compared to a pattern calculated using results from the crystal-structure analysis and the program CRYSCON (Dowty 2002) and overall, there is a good agreement between the two (Table[1] 3). It is worth noting that charleshatchettite and hochelagaite have significantly different PXRD patterns (Table 3), making distinguishing between them straightforward and supporting them as being distinct species.

To obtain a crystal suitable for single-crystal XRD, individual crystals were separated from a coarse-grained, charleshatchettite-bearing globule and examined optically with a polarizing-light microscope. From these, a crystal with the dimensions 0.09 × 0.03 × 0.01 mm, exhibiting a simple extinction and no evidence for twinning was selected. X-ray intensity data were collected on a Bruker D8 three-circle diffractometer equipped with a rotating-anode generator, multi-layer optics incident beam path and an APEX-II CCD detector. X-ray diffraction data were collected to 60° 2θ using 20 s per 0.3° frame and with a crystal-to-detector distance of 5 cm. The unit-cell parameters for charleshatchettite, obtained by least-squares refinement of 4160 reflections ($I > 10\sigma I$), are a = 21.151(4), b = 6.496(2), c = 12.714(3) Å, and β = 103.96(3)° (Table 4), are very similar to those of hochelagaite (Table 5). An empirical absorption correction (SADABS; Sheldrick 1997) was applied and equivalent reflections merged to give 1106 unique reflections covering the entire Ewald sphere.

Solution and refinement of the crystal structure of charleshatchettite were done using SHELXL-97 (Sheldrick 1997). The crystal structure was solved using direct methods, using the scattering curves of Cromer and Mann (1968) and the scattering factors of Cromer and Liberman (1970). Phasing of a set of normalized structure factors gave a mean value of $|E^2 - 1|$ value of 0.908, consistent with a center of symmetry being present ($|E^2 - 1|$ = 0.968 for centrosymmetric, $|E^2 - 1|$ = 0.736 for non-centrosymmetric). Based on this and the space-group choices available, *C*2/*c* (no. 15) was chosen as the correct space group. Phase-normalized structure factors were used to give a Fourier difference map from which two *Nb*, and several *O* sites were located. The *Ca* site and additional *O* sites were identified from subsequent Fourier difference maps. Refinement of the site-occupancy factors (SOF) indicated that all of the cation and anion sites were fully occupied (Table[1] 6). Determination of which *O* sites were occupied by OH or H_2O was based on a bond-valence analysis (Table 7). Some of the *O* sites were found to have low bond-valence sums (i.e., BVS = 1.500–1.800 v.u.) probably due to the presence of OH at these sites. Hydrogen sites were located for OH as well as the OW7, OW8, and OW10 groups however, the H atom sites could not be located for the OW9 site. This is due to the positional disorder of the oxygen associated with OW9. Refinement of this final model converged to R = 5.39% and wR^2 = 13.89%. CIF is available[1].

TABLE 4. Miscellaneous single-crystal data for charleshatchettite

a (Å)	21.151(4)	Monochromator	Graphite
b	6.496(2)	Intensity-data collection	θ:2θ
c	12.714(3)	Criterion for observed	
β (°)	103.96(3)	reflections	$F_o > 4\sigma(F_o)$
V (Å^3)	1695.3(6)	GooF	1.188
Space group	*C*2/*c* (#2)	Total no. of reflections	4160
Z	4	No. unique reflections	1106
D_{calc} (g/cm^3)	2.878	R (merge %)	7.85
Radiation	Mo*K*α (50 kV, 40 mA)	R %	5.39
		wR^2 %	13.89

TABLE 5. Crystallographic parameters for members of the franconite group

	Charleshatchettite	Hochelagaite[a]	Franconite[b]	Ternovite[c]
a (Å)	21.151(4)	19.88(1)	10.119(2)	20.656
b (Å)	6.496(2)	12.83(1)	6.436(1)	13.062
c (Å)	12.714(3)	6.44(1)	12.682(2)	6.388
β (°)	103.96(3)	93.20(3)	99.91(3)	90.917
V (Å^3)	1695.3(6)	1655.89(1)	813.6(1)	1709.83
Z	4	4	4	4
Space group	*C*2/*c* (#15)	unknown	$P2_1/c$	*P*2/*m*, *P*2, *Pm*

[a] Jambor et al. (1986).
[b] Haring and McDonald (2014).
[b] Subbotin et al. (1997).

TABLE 7. Bond-valence table (v.u.) for charleshatchettite

	Ca	Nb1	Nb2	Σ
O1		1.537$^{\downarrow\rightarrow}$		1.537
O2		0.930$^{\downarrow\rightarrow}$	0.841$^{\downarrow\rightarrow}$	1.771
O3		0.763$^{\downarrow\rightarrow}$	1.245$^{\downarrow\rightarrow}$	2.008
O4		0.817$^{\downarrow\rightarrow}$	0.853$^{\downarrow\rightarrow}$	1.670
O5		0.780$^{\downarrow\rightarrow}$	1.265$^{\downarrow\rightarrow}$	2.045
OH6		0.312$^{\downarrow\rightarrow}$	0.784$^{\downarrow\rightarrow}$	1.096
OW7	0.480$^{\downarrow\rightarrow}$			0.480
OW8	0.498$^{\downarrow\rightarrow}$			0.498
OW9*a*	0.328$^{\downarrow\rightarrow}$			0.328
OW9*b*	0.178$^{\downarrow\rightarrow}$			0.178
OW10	0.408$^{\downarrow\rightarrow}$			0.408
Σ	1.891	5.139	4.988	

DESCRIPTION OF CRYSTAL STRUCTURE

Cation polyhedra

The crystal structure of charleshatchettite contains one unique *Ca* site and two *Nb* sites. Results from the refined-crystal structure and EMPA data indicate that both the *Ca* and *Nb* sites are fully occupied. The *Ca* site is [8]-coordinated by four crystallographically distinct H_2O groups, forming $Ca(H_2O)_8$ polyhedron. Of the H_2O groups, one in particular, OW9, showed a pronounced electron density spread of 0.64 Å along [010]; it was subsequently modeled as a split site, OW9a and OW9b (Table[1] 6). Refinement of this model gave SOFs of 0.63(2) and 0.37(3) for the two split sites, suggesting a relatively high de-

[1]Deposit item AM-17-115926, Tables 3 and 6; CIF. Deposit items are free to all readers and found on the MSA web site, via the specific issue's Table of Contents (go to http://www.minsocam.org/MSA/AmMin/TOC/2017/Nov2017_data/Nov2017_data.html).

TABLE 8. Interatomic distances (Å) in charleshatchettite

Ca$(H_2O)_8$ Polyhedron		*Nb*(2)$O_4(OH)_2$ Octahedron	
Ca–OW9*b* ×2	2.66(7)	*Nb*2–O3	1.828(9)
Ca–OW9*a* ×2	2.40(4)	*Nb*2–O5	1.823(9)
Ca–OW7 ×2	2.49(2)	*Nb*2–O4	1.969(9)
Ca–OW8 ×2	2.48(2)	*Nb*2–O2	1.972(9)
Ca–OW10 ×2	2.56(2)	*Nb*2–OH6	2.248(9)
<*Ca*–O>	2.518	*Nb*2–OH6	2.281(9)
		<*Nb*2–O>	2.020
Nb(1)O_5(OH) Octahedron			
*Nb*1–O1	1.749(2)		
*Nb*1–O2	1.936(9)		
*Nb*1–O5	2.004(8)		
*Nb*1–O4	1.985(8)		
*Nb*1–O3	2.012(9)		
*Nb*1–OH6	2.352(9)		
<*Nb*1–O>	2.006		

gree of disorder for the OW9 site. There are two *Nb* sites both in octahedral coordination with O atoms and OH groups: Nb(1)O_5(OH) and Nb(2)$O_4(OH)_2$. The two Nb polyhedra are highly distorted with Nb-(O,OH) bond lengths ranging from 1.749(2) to 2.352(9) and 1.823(9) to 2.281(9) Å, respectively (Table 8); this range is consistent with the range in Nb-O bond distances previously observed in franconite (Haring and McDonald 2014) and in other Nb-bearing minerals. These distorted octahedra are likely the result of edge-sharing Nb octahedra (see discussion below), which contain a highly charged cation. In both Nb polyhedra, the longest bonds are associated with Nb-OH bonds, whereas the shortest bonds are associated with Nb-O bonds.

Bond topology

The Nb polyhedra are linked through shared edges to form four-membered clusters composed of two Nb(1)O_5(OH) and two Nb(2)$O_4(OH)_2$ octahedra (Fig. 5). Each cluster is subsequently linked to six adjacent clusters through shared corners generating 4 × 4 Å pore spaces and forming infinite sheets parallel to [100]. The sheets parallel to [100] correlate with the flattened aspect of crystals and the perfect cleavage in that direction. The layers of Nb(O,OH)$_6$ octahedra alternate with those containing Ca$(H_2O)_8$ polyhedra along [100] with an interlayer spacing of ~4 Å (Fig. 6).

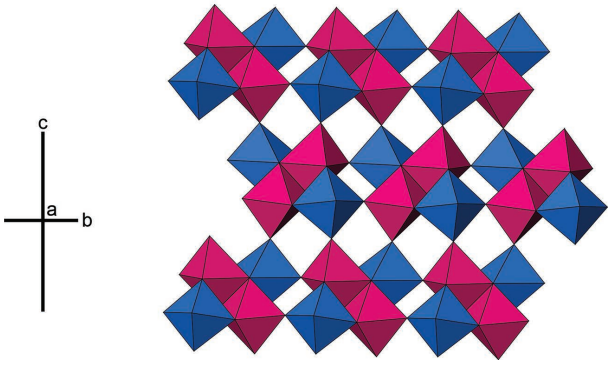

FIGURE 5. The crystal structure of charleshatchettite viewed along [100]. The Nb(1)O_5(OH) (blue) and Nb(2)$O_4(OH)_2$ (pink) octahedra are linked through shared edges to form four-membered clusters. The clusters are then joined through shared corners to adjacent ones, leading to development of infinite sheets in the *b*-*c* plane. (Color online.)

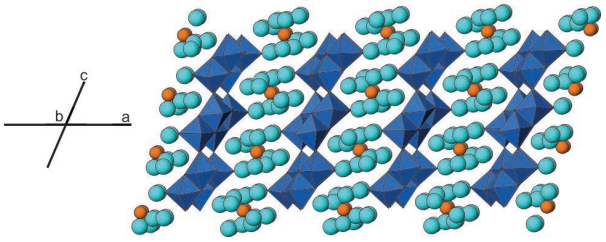

FIGURE 6. The crystal structure of charleshatchettite viwed along [010]. Layers composed of Nb(O,OH)$_6$ octahedra alternate along [100] with layers composed of Ca atoms (orange) and H_2O (light blue). Weak H-bonding between the layers results in the perfect {100} cleavage observed in the mineral. (Color online.)

Related structures

The crystal structure of charleshatchettite is topologically similar to that of franconite (Haring and McDonald 2014). Both minerals are hydrous with an $[Nb_2O_5(OH)]^{-1}$ group, the two differing by the type of interlayer cation between the $[Nb_2O_5(OH)]^{-1}$ sheets: charleshatchettite having Ca$(H_2O)_8$ polyhedra and franconite with NaO$(H_2O)_4$ polyhedra (Haring and McDonald 2014). The presence of Ca$(H_2O)_8$ polyhedra in charleshatchettite and the flipping in the octahedral layers correlates with a doubling of the *a* dimension to 21.151 Å compared to franconite where *a* = 10.119 Å as there are additional H_2O groups coordinated with Ca compared with Na in NaO$(H_2O)_4$. Both charleshatchettite and franconite possess crystal structures with layers of *A*$(H_2O)_{5–8}$ (*A* = Na,Ca) linked to layers of Nb(O,OH)$_6$ octahedra through H-bonds along [100], the latter producing the perfect [100] cleavage observed in these minerals. Chemically, charleshatchettite [$CaNb_4O_{10}(OH)_2 \cdot 8H_2O$] most closely resembles hochelagaite ($CaNb_4O_{11} \cdot nH_2O$), but as mentioned above, the two have unique PXRD patterns (Table 3). The crystal structure of hochelagaite is unknown but is presumed to be similar to those of franconite and charleshatchettite. It is however noteworthy that the PXRD pattern for hochelagaite has systematic extinctions that support the mineral having a *P*-lattice, which is different from the *C*-lattice in charleshatchettite. The difference in lattice types between the two may be attributed to the higher proportion of H_2O groups in charleshatchettite relative to hochelagaite.

The crystal structure of charleshatchettite is broadly similar to those of the synthetic compounds $Na_2Nb_4O_{11}$ (Masó et al. 2011) and $KCa_2Nb_3O_{10}$ (Fukoka et al. 2000; Jehng and Wachs 1990) and SOMS [$Na_2Nb_{2-x}Ti_xO_{6-x}(OH)_x \cdot H_2O$ (x = 0.04 to 0.40); Nyman et al. 2001]. These compounds have strongly layered structures where layers of Nb(O,OH)$_x$ (X = 6 or 7) polyhedra alternate with layers of *M*O$_x$ (X = 6 or 7; *M* = Na, K, and Ca) polyhedra. Both SOMS and $Na_2Nb_4O_{11}$, like charleshatchettite, are monoclinic in symmetry and crystallize in the space group *C*2/*c* (Nyman et al. 2001; Masó et al. 2011), whereas $KCa_2Nb_3O_{10}$ is orthorhombic, crystallizing in the space group *Cmcm* (Fukoka et al. 2000). Unlike the structures of SOMS and charleshatchettite, $KCa_2Nb_3O_{10}$ is considered to have a layered perovskite-type structure where slabs of corner-sharing NbO_6 octahedra and Ca ions alternate along [010] with layers of K ions (Fukoka et al. 2000). In the case of $Na_2Nb_4O_{11}$, layers of edge-sharing (Nb,Ta)O_7 polyhedra alternate with layers composed of edge-sharing NaO_7 and

$(Nb,Ta)O_6$ polyhedra (Masó et al. 2011). Of the synthetic compounds, charleshatchettite is most crystallochemically similar to SOMS. The crystal structures of SOMS contain NbO_6 polyhedra consisting of a short bond of ~1.8 Å, a long bond of ~2.4 Å as well as four equatorial bonds with distances of ~2 Å (Nyman et al. 2002), similar to the $Nb(1)O_5(OH)$ polyhedra in charleshatchettite. These NbO_6 octahedra, like those in charleshatchettite, form four-membered clusters through shared edges. Adjacent four-membered NbO_6 clusters do not link to form infinite NbO_6 sheets as in charleshatchettite, but are instead linked to double chains of NaO_6 octahedra through shared edges. The four-membered NbO_6 clusters and NaO_6 double chains occur in discreet layers, which alternate with one another along [001] (Xu et al. 2004). As in charleshatchettite, the crystal structures of SOMS are linked together in part by H-bonds and are able to adsorb extra water into its structure. The amount of H-bonding in the structures of SOMS increase with increasing Ti substitution for Nb due to the substitution reaction $Ti^{4+} + OH^- \leftrightarrow Nb^{5+} + O^{2-}$, whereby more OH groups are added with the addition of Ti into the structure (Nyman et al. 2002). The compounds $Na_2Nb_4O_{11}$ and $KCa_2Nb_3O_{10}$ have been synthesized at high temperatures (~1100–1300 °C) while SOMS have been hydrothermally synthesized under conditions of at low T (~175 °C) and high alkalinity (pH ~ 13.7) (Xu et al. 2004). However, increasing the Ti content in SOMS increases the range in T over which the structures are stable: a 20% Ti substitution for Nb results in the structures being stabilized up to 576 °C (Nyman et al. 2002). The compounds $Na_2Nb_4O_{11}$ and $KCa_2Nb_3O_{10}$ have distinct ferroelectric and dielectric properties (Masó et al. 2011; Yim et al. 2013). On the other hand, SOMS exhibit a strong ion-exchange selectivity for R^{2+} cations over R^+ cations, making them useful in removing heavy metals such as Pb^{2+}, Co^{2+}, and Cd^{2+} from ground water and soils (Nyman et al. 2001), these being trapped in pores of the Nb clusters. Due to the strong crystallochemical similarities between charleshatchettite and SOMS, charleshatchettite is expected to have similar cation exchange properties. Such cation exchange properties are supported by the range of chemistries observed for FGM [i.e., incorporation of Na, Ca, Mg, ±Sr, and $\pm Fe^{2+}$ into FGM structures (Jambor et al. 1984, 1986; Subbotin et al. 1997; Haring and McDonald 2014)].

Origin and conditions of formation

Paragenetically, charleshatchettite is a late-stage phase found overgrowing earlier formed phases including, albite, quartz, siderite, muscovite, pyrrhotite, and ancylite-(Ce). The mineral, due its hydrous composition, is inferred to have precipitated from aqueous fluids. Previous studies of franconite and hochelagaite, using results from microprobe and mass spectrometry, have shown that the water content can be variable in these minerals, with the number of H_2O groups (apfu) ranging from 3–26 for franconite and 3–9 for hochelagaite (Jambor et al. 1984, 1986). Previous heating experiments of Jambor et al. (1984) on franconite to temperatures of 150, 250, 350, and 500 °C coupled with PXRD data, reveal a gradual collapse of the structure up to 500 °C at which point the material was found to give a PXRD consistent with that of $Na_2Nb_4O_{11}$. The collapse of the franconite structure is attributed to the loss of H_2O groups: the removal of H_2O groups would result in the loss of H-bonding that bind layers of $Nb(O,OH)_6$ octahedra to layers of $Na(O,H_2O)_5$ polyhedra, thus leading to structural collapse. As H-bonds are essential in stabilizing the crystal structure of franconite, they are also inferred to be equally important in stabilizing the crystal structure of charleshatchettite. It follows, therefore, that heating of charleshatchettite should also lead to a collapse in the crystal structure similar to that observed to in franconite. Given the ease with which franconite loses its structurally bound H_2O and the fact that charleshatchettite shows a greater degree of hydration (H_2O_{calc} = 22.96 wt%) relative to hochelagaite (H_2O_{calc} = 13.20 wt%), it is possible that charleshatchettite formed at either a lower T (<150 °C) or under conditions of higher a_{H_2O}, relative to hochelagaite. The presence of coexisting siderite and pyrrhotite suggest that the fluids were slightly reducing (Eh = 0.0 to –0.4) with a neutral to slightly basic pH (pH = 7 to 8) [at a T of 25 °C] (Vaughan 2005; Faure 1991). Due to the crystallochemical similarities between charleshatchettite and SOMS and the fact that SOMS are synthesized at a very high pH, it is probable that the fluids from which charleshatchettite precipitated were also highly alkaline.

Genetic implications

Charleshatchettite has strong crystallochemical similarities to other Franconite-group minerals (FGM) and as such should be considered a new member. This broadens the number of related minerals and demonstrates the crystal-chemical flexibility of the FGM crystal structure. Although the crystal structures of the FGM are flexible, no Ti- or Zr-dominant members of the FGM have been found to date, despite Ti and Zr having valences and atomic radii ($^{[6]}Ti^{4+}$ = 0.61 Å, $^{[6]}Zr^{4+}$ = 0.72 Å) similar to those of Nb ($^{[6]}Nb^{5+}$ = 0.64 Å) (Shannon 1976). The SOMS can incorporate other high-field strength elements like Ti and Zr through the substitution: Ti^{4+} (or Zr^{4+}) + $OH^- \leftrightarrow Nb^{5+} + O^{2-}$ (Nyman et al. 2002; Xu et al. 2004). In light of the crystal-chemical similarities between SOMS and charleshatchettite, the occurrence of Ti- or Zr-dominant FMG would seem plausible; however, such phases have yet to be discovered. It is noteworthy that the crystal structure of SOMS can only incorporate up to 20% Ti or Zr after which the octahedral sites become increasingly distorted and disordered as observed in the broadening of octahedral peaks in the infrared spectrum of SOMS (Nyman et al. 2002). The degree of Ti/Nb substitution in FGM varies from 0.25 to 8.00%, suggesting that a similar distortion and disordering of the octahedral sites may occur in charleshatchettite; this may thus preclude the crystallization of Ti- and Zr-rich members of the FGM. Incorporation of Ti may also proceed through the substitution $Ti^{4+} + OH^- \leftrightarrow Nb^{5+} + O^{2-}$; such a substitution in charleshatchettite is supported by the fact that some of the O sites are have low bond-valence sums (i.e., BVS ~1.5–1.8 v.u.), suggesting the presence of mixed O/OH sites.

Charleshatchettite is a late-stage mineral that probably developed from a Nb-rich precursor that would have been unstable in the presence of highly alkaline, slightly reducing, aqueous fluids. Presumably, the precursor mineral itself would have been both Nb-dominant and virtually devoid of Ta, similar to the chemistry of charleshatchettite. A similar paucity of Ta is observed in other Nb-rich minerals such as vuonnemite $[Na_{11}Ti^{4+}Nb_2(Si_2O_7)_2(PO_4)_2$

$O_3(F,OH)$; Ercit et al. 1998], epistolite $[Na_4Nb_2Ti^{4+}(Si_2O_7)_2O_2(OH)_2(H_2O)_4$; Sokolova and Hawthorne 2004], laurentianite $\{[NbO(H_2O)]_3(Si_2O_7)_2[Na(H_2O)_2]_3$; Haring et al. 2012$\}$, and franconite $[NaNb_2O_5(OH)\cdot 3H_2O$; Haring and McDonald 2014], laurentianite (from agpaitic environments) suggesting that Ta and Nb must undergo significant fractionation prior to late-stage crystallization in agpaitic environments. Possible precursor minerals to charleshatchettite include pyrochlore- or eudialyte-group minerals or possibly vuonnemite. Interactions of fluids with these precursor minerals, especially vuonnemite, which is highly susceptible to weathering (Khomyakov et al. 1975b; Bussen et al. 1978), would have led to an Nb-enrichment of these the fluids. Evidence for the mobility of Nb in agpaitic environments can be seen in the paragenetic relationship between the Nb minerals laurentianite ($[NbO(H_2O)]_3(Si_2O_7)_2[Na(H_2O)_2]_3$) and franconite, whereby laurentianite overgrows the latter (Haring et al. 2012). In addition to Nb-enrichment, these fluids could have also been enriched in Ca possibly due to interaction with the carbonate rocks into which the Mont Saint-Hilaire syenites intruded.

Acknowledgments

Our thanks to F.C. Hawthorne (Department of Geological Sciences, University of Manitoba) for providing access to the four-circle diffractometer and to Mark C. Cooper for providing assistance with the single-crystal XRD data collection. In addition, we thank Joy Gray-Munro (Department of Chemistry and Biochemistry, Laurentian University) for providing access to the infrared spectrometer as well as assistance with the data collection. We also acknowledge the comments made by Anthony Kampf and those of the associate editor, Beda Hofmann. Financial support for this research was provided through a grant to A.M.M. from the Natural Sciences and Engineering Research Council as well as an Alexander Graham Bell Canada Graduate Scholarship to M.M.M.H. also from the Natural Sciences and Engineering Research Council.

References cited

Belovitskaya, Y.V. and Pekov, I.V. (2004) Genetic mineralogy of the burbankite group. New Data on Minerals, 39, 50–64.

Bussen, I.V., Es'kova, E.M., Men'shikov, Yu.P., et al. (1978) The mineralogy of hyperalkaline pegmatites. Problems of Geology of Rare Elements, M., 251–271.

Cromer, D.T., and Liberman, D. (1970) Relativistic calculation of anomalous scattering factors for X-rays. Journal of Physical Chemistry, 53, 1891–1898.

Cromer, D.T., and Mann, J.B. (1968) X-ray scattering factors computed from numerical Hartree-Frock wave functions. Acta Crystallographica, A24, 321–324.

Cooper, M.A., and Hawthorne, F.C. (2012) The crystal structure of kraisslite, $^{[4]}Zn_3(Mn,Mg)_{25}(Fe^{3+},Al)(As^{3+}O_3)_2[(Si,As^{5+})O_4]_{10}(OH)_{16}$, from the Sterling Hill mine, Ogdensburg, Sussex County, New Jersey, USA. Mineralogical Magazine, 76, 2819–2836.

Dowty, E. (2002) CRYSCON for Windows and Macintosh Version 1.1. Shape Software Kingsport, Tennessee, U.S.A.

——— (2009) VIBRATZ for Windows and Macintosh Version 2.2. Shape Software Kingsport, Tennessee, U.S.A.

Ercit, T.S., Cooper, M.A., and Hawthorne, F.C. (1998) The crystal structure of vuonnemite, $Na_{11}Ti^{4+}Nb_2(Si_2O_7)_2(PO_4)_2O_3(F,OH)$, a phosphate-bearing sorosilicate of the lomonosovite group. Canadian Mineralogist, 36, 1311–1320.

Faure, G. (1991) Principles and Applications of Geochemistry, 2nd ed. Prentice Hall, p. 243.

Fielicke, A., Meijer, G., and Von Helden, G. (2003) Infrared spectroscopy of niobium oxide cluster cations in a molecular beam: identifying the cluster structures. Journal of the American Chemical Society, 125, 3659–3667.

Frisch, M.J., Trucks, G.W., Schlegel, H.B., et al. (2013) Gaussian 09, Revision D.01. Gaussian, Inc., Wallingford, Connecticut.

Fukoka, H., Isami, T. and Yamanaka, S. (2000) Crystal structure of a layered perovskite niobate $KCa_2Nb_3O_{10}$. Journal of Solid State Chemistry, 151, 40–45.

Haring, M.M., and McDonald, A.M. (2014) Franconite, $NaNb_2O_5(OH)\cdot 3H_2O$: Structure determination and the role of H bonding, with comments on the crystal chemistry of franconite-related minerals. Mineralogical Magazine, 78, 591–607.

Haring, M.M.M., McDonald, A.M., Cooper, M.A., and Poirier, G.A. (2012) Laurentianite, $[NbO(H_2O)]_3(Si_2O_7)_2[Na(H_2O)_2]_3$, a new mineral from Mont Saint-Hilaire, Québec: Description, crystal-structure determination and paragenesis. Canadian Mineralogist, 50, 1265–1280.

Horváth, L., and Gault, R.A. (1990) The mineralogy of Mont Saint-Hilaire Québec. Mineralogical Record, 21, 284–359.

Horváth, L., Pfenninger Horváth, E., Gault, R.A., and Tarasoff, P. (1998) Mineralogy of the Saint-Amable sill, Varennes and Saint-Amable Quebec. Mineralogical Record, 29, 83–118.

Jambor, J.L., Sabina, A.P., Roberts, A.C., Bonardi, M., Owens, D.R., and Sturman, B.D. (1986) Hochelagaite, a new calium-niobium oxide mineral from Montreal, Québec. Canadian Mineralogist, 24, 449–453.

Jambor, J.L., Sabina, A.P., Roberts, A.C., Bonardi, M., Ramik, R.R., and Sturman B.D. (1984) Franconite, a new hydrated Na-Nb oxide mineral from Montreal Island, Québec. Canadian Mineralogist, 22, 239–243.

Jehng, J.M., and Wachs, I.E. (1990) Structural chemistry and Raman spectra of niobium oxides. Chemistry of Materials, 3, 101–107.

Khomyakov, A.P., Semenov, E.I., Es'kova, E.M., et al. (1975b) Vuonnemite from Lovozero. Iz.AN, ser.geol, 8, 78–87.

Kontny, A., de Wall, H., Sharp, T.G., and Posfai, M. (2000) Mineralogy and magnetic behavior of pyrrhotite from a 260 °C section at the KTB drilling site, Germany. American Mineralogist, 85, 1416–1427.

Mandarino, J.A. (1981) The Gladstone-Dale relationship. IV. The compatibility concept and its application. Canadian Mineralogist, 19, 441–450.

Masó, N., Woodward, D.I., Várez, A., and West, A.R. (2011) Polymorphism, structural characterization and electrical properties of $Na_2Nb_4O_{11}$. Journal of Material Chemistry, 21, 12096–12102.

Nikandrov, S.N. (1990) Franconite, first find in the USSR. Doklady Akademii Nauk SSSR, 305, 700–703.

Nyman, M., Tripathi, A., Parise, J.B., Maxwell, R.S., Harrison, W.T.A., and Nenoff, T.M. (2001) A new family of octahedral molecular sieves: Sodium Ti/Zr^{IV} niobates. Journal of the American Chemical Society, 123, 1529–1530.

Nyman, M., Tripathi, A., Parise, J.B., Maxwell, R.S., and Nenoff, T.M. (2002) Sandia octahedral molecular sieves (SOMS): Structural and property effects of charge-balancing the M^{IV}-substituted (M = Ti, Zr) niobate framework. Journal of the American Chemical Society, 124, 1704–1713.

Pekov, I.V., and Podlesnyi, A.S. (2004) Kukisvumchorr deposit: Mineralogy of alkaline pegmatites and hydrothermalites. Mineralogical Almanac, 7, 168.

Shannon, R.D. (1976) Revised effective ionic radii and systematic studies in interatomic distances in halides and chalogenides. Acta Crystallographica, A32, 751–767.

Sheldrick, G.M. (1997) SHELXL-97: A computer program for the refinement of crystal structures. University of Göttingen, Göttingen, Germany.

Sokolova, E., and Hawthorne, F.C. (2004) The crystal chemistry of epistolite. Canadian Mineralogist, 42, 797–806.

Subbotin, V.V., Voloshin, A.V., Pakhomovskii, Y.A., Men'shikov, Y.P., and Subbotina, G.F. (1997) Ternovite, $(Mg,Ca)Nb_4O_{11}\cdot nH_2O$, a new mineral and other hydrous tetraniobates from carbonatites of the Vuoriyarvi massif, Kola Peninsula, Russia. Neues Jahrbuch für Mineralogie, 2, 49–60.

Vaughan, D.J. (2005) Minerals/Sulphides. Encyclopedia of Geology, Elsevier, 574–586.

Williams, Q. (1995) Infrared, Raman and optical spectroscopy of Earth materials. In T.J. Ahrens, Ed., Mineral Physics and Crystallography: A handbook of physical constants. AGU Reference Shelf Vol 2., 291–302 American Geophysical Union, Washington, D.C.

Xu, H., Nyman, M., Nenoff, T.M., and Navrotsky, A. (2004) Prototype Sandia Octahedral Molecular Sieve (SOMS) $Na_2Nb_2O_6\cdot H_2O$: Synthesis, structure, and thermodynamic stability. Chemistry of Materials, 16, 2034–2040.

Yim, H., Yoo, S., Nahm, S., Hwang, S., Yoon, S., and Choi, J. (2013) Synthesis and dielectric properties of layered $HCa_2Nb_3O_{10}$ structure ceramics. Ceramics International, 39, 611–614.

Manuscript received August 2, 2016
Manuscript accepted June 29, 2017
Manuscript handled by Fabrizio Nestola